Global bifurcation criterion for oscillatory crack path instability

Van-Bac Pham,[1,*] Hans-Achim Bahr,[1] Ute Bahr,[2] Herbert Balke,[1] and Hans-Jürgen Weiss[3]
[1]*Institut für Festkörpermechanik, Technische Universität Dresden, D-01062 Dresden, Germany*
[2]*Institut für Theoretische Physik, Technische Universität Dresden,D-01062 Dresden, Germany*
[3]*Fraunhofer-Institut für Werkstoff- und Strahltechnik, D-01277 Dresden, Germany*
(Received 13 August 2007; revised manuscript received 19 December 2007; published 27 June 2008)

A bifurcation criterion for the transition from straight to oscillatory quasistatic crack propagation in an isotropic material is derived from the requirement of pure mode I stress fields at the crack tip ($K_{II}=0$) on the entire crack path, henceforth called global bifurcation criterion. For a small-amplitude sine-shaped crack path which is observed in experiments at the transition, it is shown to be sufficient to postulate $K_{II}=0$ only for two phases of the crack path instead, which simplifies calculations. By using the measured temperature fields to solve the thermoelastic problem of dipping a hot thin glass slab into cold water, critical wavelengths of the oscillating crack growth obtained with the derived global bifurcation criterion agree remarkably well with those observed in experiments by Ronsin and Perrin. It is also shown that local bifurcation criteria, which do not take into account $K_{II}=0$ on the entire crack path, lead to incorrect results for the oscillatory crack path instability.

DOI: 10.1103/PhysRevE.77.066114 PACS number(s): 46.50.+a, 62.20.M−, 81.40.Np

I. INTRODUCTION

Quasistatic oscillatory crack propagation is a prime example for crack path instability which has been intensively investigated in the last decade. In an interesting simple experiment, Yuse and Sano [1] produced reproducible controlled quasistatic crack propagation due to thermal stresses by dipping a hot thin soda-lime glass slab with constant velocity v into cold water (Fig. 1).

The temperature gradient induces a stress field in the vicinity of the cooling front which drives the crack to propagate. Depending on the parameters velocity v and temperature difference ΔT between the oven and the bath, and by keeping constant the slab width L, they observed different crack morphology: no crack propagation, straight crack, oscillatory single, and branched crack. Since then, the experiment was repeatedly modified by Ronsin *et al.* [2], Ronsin and Perrin [3,4], Yuse and Sano [5], and Ferney *et al.* [6].

The attention in many experimental and analytical works is paid to the conditions for the transition from one crack morphology to another. In this paper we solely focus on the transition from straight to oscillatory crack propagation as an important, particular directional instability phenomenon of the crack path.

If the control parameters v, ΔT, and L are small, the straight crack on the specimen center is the stable solution. By increasing these parameters, the oscillatory crack propagation is a result of two competing effects. A crack on the specimen center tends to break out of the symmetrical line because the straight crack is the unstable solution. After breaking out, the interaction with the free boundaries of the specimen drives the crack back. These procedures recur; and the crack oscillates around the center line. Depending on the above parameters this oscillation can decay or build up.

The onset of the oscillatory crack propagation called oscillatory crack path instability or oscillatory instability can be defined as the transition from decaying to growing amplitude of the disturbed crack path. The determination of this morphological phase boundary between straight and undulating crack paths was the goal of many investigations in the literature.

First attempts were made by Furukawa [7] and Hayakawa [8] by using a deterministic spring network model. Numerous following theoretical and numerical analyses in the framework of continuum theory used a local bifurcation criterion by consideration of only one crack tip position: Marder [9], Adda-Bedia and Pomeau [10], Ferney *et al.* [6], Yang and Ravi-Chandar [11], and recently Bouchbinder *et al.* [12]. Sumi *et al.* [13,14] tried to extend the examined crack path to an "intermediate" range. However, for the crack path prediction the near-tip stress fields were used, which restricts the validity range of the solution.

Other works considered the entire crack path in all phases henceforth called global analysis. Sasa *et al.* [15] examined the long time behavior of the crack tip position. But they applied an "infinite plate approximation" for the calculation of the stress intensity factors. Global consideration of the crack path was done by Bahr *et al.* [16,17] using simulation with finite element method (FEM) and in Refs. [18–20] using a global bifurcation analysis, see Eq. (8).

In spite of many investigations, the phenomenon of oscillatory instability is not understood completely, as will be summarized in the following. Marder [9] calculated the frac-

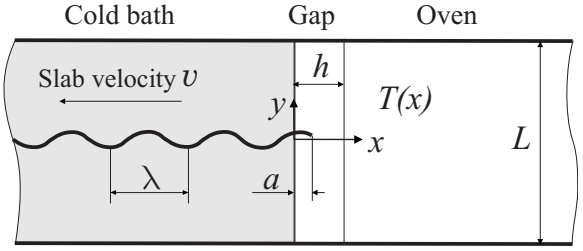

FIG. 1. Experiment by Yuse and Sano [1].

*van_Bac.Pham@tu-dresden.de

ture energy of soda-lime glass at the transition from straight to oscillatory crack propagation predicted by the T criterion of Cotterell and Rice [21]. The plane stress fields near the crack tip in the polar coordinate system (r,θ) with $\theta=0$ being the tangent direction and the origin at the crack tip take the general form

$$\sigma_{ij} = \frac{1}{\sqrt{2\pi r}}[K_{\mathrm{I}} f_{ij}^{(\mathrm{I})}(\theta) + K_{\mathrm{II}} f_{ij}^{(\mathrm{II})}(\theta)]. \tag{1}$$

$K_{\mathrm{I}}, K_{\mathrm{II}}$ are the modes I and II stress intensity factors (SIFs), respectively, and $f_{ij}^{(\mathrm{I})}(\theta), f_{ij}^{(\mathrm{II})}(\theta)$ the universal angular functions common to all loadings and geometries. The so-called T stress, the next, nonsingular term of the Williams expansion [22] representing the uniform stress acting parallel to the crack at its tip, was determined by Marder for the straight crack as a function of the position of the crack tip a relative to the cold front (see Fig. 1). The cold front means the water surface of the bath. The T criterion implies that the crack becomes directionally unstable when the crack tip passes the location where the T stress changes from negative to positive. Applying the T criterion for the onset of the oscillatory crack instability in the experiments of Yuse and Sano [1], Marder [9] found a strong velocity dependence of the fracture energy of glass. This, however, is not justified physically in the low range of crack speeds in the experiments.

Adda-Bedia and Ben Amar [23] also concluded the applicability of the T criterion for the change from straight to wavy crack propagation. Sasa *et al.* [15], Ronsin *et al.* [2], and Yang and Ravi-Chandar [11] noticed that the T criterion does not work for the prediction of the oscillatory instability. As commonly assumed in the literature, this is thought to be brought about by finite geometry, which is an unsatisfactory explanation. Furthermore, the definition of a divergence point as the bifurcation point as introduced in Ref. [11] is not adequate.

Recently we investigated curved crack paths with attention to the two limiting situations: the initial crack path after a disturbance to verify the Cotterell and Rice solution, and the asymptotic one to study the global directional stability of crack paths in general [24]. The smooth cracks in isotropic material are assumed to obey the local symmetry everywhere. That means that the mode II stress singularity factor vanishes along the entire smooth crack path:

$$K_{\mathrm{II}} = 0. \tag{2}$$

If $K_{\mathrm{II}} \neq 0$ at the crack tip, the crack would abruptly change its direction; the crack path would exhibit a kink at this position, and hence it would not be smooth [21]. By driving a curved crack straightly in the tangent direction at the crack tip the local symmetry (2) will be broken ($K_{\mathrm{II}} \neq 0$). The change of $K_{\mathrm{II}}(s)$ along a straight extension s in the tangent direction determines the curvature C of the crack path according to Amestoy and Leblond [see Eq. (104) in Ref. [25]]

$$C = -\frac{2}{K_{\mathrm{I}}}\left[\frac{dK_{\mathrm{II}}(s)}{ds}\right]_{\mathrm{straight}}. \tag{3}$$

Our procedure for the simulation of curved crack propagation used in [24] corresponds to Eq. (3).

The principle of local symmetry for plane curvilinear cracks was first formulated by Barenblatt and Cherepanov [26,27], as well as by Erdogan and Sih [28], and generalized for three-dimensional cracks by Gol'dstein and Salganik [29]. For isotropic material and brittle fracture (small scale yielding), it is consistent with the criterion of maximum energy release rate and other known criteria [21]. To our knowledge, it is the most widely accepted criterion [9,15,21,30–32] and confirmed by experiments [33]. Note that this principle does not hold generally for crack propagation in anisotropic material.

The crack propagation starts and continues as long as the condition

$$K_{\mathrm{I}} = K_{\mathrm{I}c} \tag{4}$$

is met. Here $K_{\mathrm{I}c}$ is the critical stress intensity factor or the fracture toughness. Our analyses [24] showed that the Cotterell and Rice solution is universal for all loading and geometrical situations if only the initial crack growth is of interest. That means that the Cotterell and Rice solution and the T criterion are valid for an amount of crack growth after a disturbance, which is small in comparison with a characteristic length, e.g., the crack length. From the initial behavior of the crack after the disturbance, however, it cannot be concluded whether the crack path oscillation is increasing or decreasing. Therefore, the transition from straight to oscillating crack (the onset of global directional crack path instability) cannot be determined with the T criterion. Indeed, any *local criterion* based on a local consideration of the crack path cannot correctly provide the transition from straight to oscillatory crack propagation.

Also the "intermediate" range of stability by Sumi [14] is not sufficient for this problem because of the small validity range of the crack path solution by using the near-tip stress fields. The criterion postulated by Adda-Bedia and Pomeau [10] (in the following abbreviated as AP criterion) is a local one, too. They considered only one phase of the sine configuration [see in Eq. (6), $\varphi=0$]:

$$K_{\mathrm{II}} = 0, \quad \frac{\partial K_{\mathrm{II}}}{\partial \lambda} = 0. \tag{5}$$

The postulation of the extremum of K_{II} by variation of λ is explained in Ref. [10] with the first instant of fulfilling the condition $K_{\mathrm{II}}=0$ for this crack tip position with increasing load parameters. This specific crack tip position is chosen rather arbitrarily. Yang and Ravi-Chandar [11] also noticed that the dependence of the results on the phase angle was not considered.

Nevertheless, by applying a criterion that is identical to this local criterion of Adda-Bedia and Pomeau, Bouchbinder *et al.* [12] have lately found a good quantitative agreement with the experiments of Ronsin and Perrin [4]. However, the temperature distribution they used for their analysis is not the realistic temperature field, as usual in other works in the literature, even though Ronsin *et al.* [2] found out that the temperature profile essentially affects the results of the analysis.

The aim of this paper is to present a global bifurcation criterion for calculation of the conditions for this oscillating instability, which takes into account $K_{II}=0$ on the entire crack path. We will also show that the local bifurcation criterion of Adda-Bedia and Pomeau [10], which does not take into account Eq. (2) on the entire crack path, can lead to incorrect results if the measured temperature distributions are used. In our analysis we use quasistatic fields because the speed of the crack tip in the experiments (Yuse and Sano [1], Ronsin and Perrin [4]) is very low in comparison to the speed of sound in the material.

II. DERIVATION OF A GLOBAL BIFURCATION CRITERION FOR THE ONSET OF OSCILLATORY INSTABILITY

As discussed above, a local consideration or a consideration over a small range of the crack path is not sufficient to predict the onset of the oscillatory instability. The whole crack path must be considered.

An appropriate method is the simulation of crack propagation. Numerical simulation methods have been applied first by Bahr *et al.* [16–18] with a straight crack increment and later by Yang and Ravi-Chandar [11] with a curved crack increment. Starting from a primary straight crack with a slight disturbance and using the crack propagation criteria (2) and (4), an undulating crack with growing or decaying amplitude has been obtained depending on the load parameters. A crack path with decaying amplitude implies that the straight crack is stable. The transition between decrease and increase of the amplitude indicates the transition from straight to oscillating crack propagation. In addition to the critical load parameters, the analysis also provides the parameters of the wavy crack such as the wavelength λ and the distance of the crack tip a from the cold front. The disadvantage of the simulation methods is more computing time.

In this paper, we apply another method for the global analysis, the ansatz method, to derive a global bifurcation criterion for the onset of the oscillating instability. The global bifurcation criterion takes into account $K_{II}=0$ (2) on the entire crack path. The ansatz method was developed by Gerbatsch [18] and further developed by Mühle [19]. An ansatz is a form function for the solution of the problem containing one or more parameters which are to be determined. In Refs. [18] and [19] simplified temperature fields at high velocities [see Eq. (14)] were used. In the following the criterion is applied for more general temperature distributions, also for low velocities.

The straight crack path on the symmetry line is always a solution for the symmetric geometry and loading in our problem. We look for another solution in addition to the straight one, and for the conditions of its existence. Of course, the other solution, too, has to fulfill the crack propagation criteria (2) and (4) at every crack tip position.

The coordinate system moves relatively to the slab such that the cold front is always at $x=0$ and the symmetry line of the slab is at $y=0$ (see Fig. 1). Assuming small amplitude A and stationary crack tip position at $x=a$ which is allowable just beyond the onset of the oscillation we make a sinusoidal ansatz for the crack contour which was observed by Yuse and Sano [1] and Ronsin *et al.* [2]:

$$y(x) = A \sin\left[\frac{2\pi}{\lambda}(x-a)+\varphi\right]. \tag{6}$$

The crack contour is defined by the amplitude A, the wavelength λ, and the distance between the crack tip and the cold front a, which are to be determined to fulfill (2) and (4) at every phase φ.

A general temperature distribution would be given with ΔT and some characteristic lengths l_i, $i=1,2,\ldots$, e.g., the thermal diffusion length $l_1=D/v$ (with D being the thermal diffusivity) and the gap $l_2=h$ [see Fig. 1 and Eq. (15)]. Further characteristic lengths are the transition length bath/gap and gap/oven which are experimentally observed by Ronsin *et al.* [2,4]. Note that these transition lengths depend on the velocity v and ΔT.

For dimensional reasons, the SIFs can be written as

$$K_I = E\alpha\Delta T\sqrt{L}k_I, \quad K_{II} = E\alpha\Delta T\sqrt{L}k_{II}$$

with E and α being Young's modulus and thermal expansion coefficient, respectively. Equation (2) reads

$$k_{II} = k_{II}\left(\frac{A}{L},\varphi,\frac{\lambda}{L},\frac{a}{L},\frac{l_i}{L}\right) = 0 \quad \text{for} \quad \forall\,\varphi.$$

All quantities depending on the crack contour, e.g., K_{II}, are periodic functions of φ and can be expanded into Fourier series. In addition, K_{II} can be expanded in a Taylor series about the vicinity of $A/L=0$. Considering $K_{II}(A)=-K_{II}(-A)$ and due to small amplitude A for the transition from straight $(A=0)$ to oscillating crack propagation $(A\neq 0)$, we obtain

$$\begin{aligned} k_{II}\left(\frac{A}{L},\varphi,\frac{\lambda}{L},\frac{a}{L},\frac{l_i}{L}\right) &= k_{II}\left(\frac{A}{L}\sin\varphi,\frac{A}{L}\cos\varphi,\frac{\lambda}{L},\frac{a}{L},\frac{l_i}{L}\right) \\ &= \alpha_1\left(\frac{\lambda}{L},\frac{a}{L},\frac{l_i}{L}\right)\frac{A}{L}\sin\varphi \\ &\quad + \beta_1\left(\frac{\lambda}{L},\frac{a}{L},\frac{l_i}{L}\right)\frac{A}{L}\cos\varphi = 0 \quad \text{for} \quad \forall\,\varphi. \end{aligned} \tag{7}$$

Because Eq. (7) holds for every phase φ, the factors α_1 and β_1 must vanish [18]:

$$\alpha_1\left(\frac{\lambda_{osc}}{L},\frac{a_{osc}}{L},\frac{l_i}{L}\right) = k_{II}\left(\varphi=\frac{\pi}{2}\right)\frac{L}{A} = 0,$$

$$\beta_1\left(\frac{\lambda_{osc}}{L},\frac{a_{osc}}{L},\frac{l_i}{L}\right) = k_{II}(\varphi=0)\frac{L}{A} = 0 \tag{8}$$

with the critical values $\lambda=\lambda_{osc}$ and $a=a_{osc}$. In this way, it has been shown for a small-amplitude sine-shaped crack path that the condition $K_{II}=0$ is fulfilled at every phase φ if this condition is satisfied at two phases, e.g., $\varphi=0$ (sine-phase) and $\varphi=\pi/2$ (cosine-phase).

Our *global bifurcation criterion*, which takes into account $K_{II}=0$ (2) on the entire crack path, says that the transition from straight to oscillatory crack propagation is governed by

Eq. (8). Of course, the condition (4) must also be fulfilled for the growing crack. The mode I stress intensity factor can also be expanded in a Taylor series in the vicinity of $A/L=0$. With taking into account the symmetry condition $K_I(A)=K_I(-A)$ one can write

$$K_I\left(\frac{A}{L},\frac{a}{L},\ldots\right)=K_I\left(\frac{A}{L}=0,\frac{a}{L},\ldots\right)+O\left(\frac{A^2}{L^2}\right).$$

That means that K_I for the oscillating crack of small amplitude is identical to K_I for the straight crack. Then Eq. (4) takes the form

$$K_I=E\alpha\Delta T\sqrt{L}k_I\left(\frac{a_{osc}}{L},\frac{l_i}{L}\right)=K_{Ic}. \tag{9}$$

The above derivation has shown that the oscillatory crack path at the transition determined by Eqs. (8) and (9) also fulfills Eqs. (2) and (4) in every crack tip position.

Equations (8) and (9) are three coupled equations for three critical parameters at the transition from straight to wavy crack propagation. Two of them are the critical length a_{osc} and the critical wavelength λ_{osc}.

In addition, if K_{Ic} is known, one of the critical parameters ΔT_{osc}, L_{osc}, l_{1osc}, or l_{2osc} can be calculated from Eq. (9), provided that all the others are fixed and known. Note that the change of temperature profile with the velocity v has to be taken into consideration. Otherwise, K_{Ic} can be determined, if L_{osc} is measured for a given temperature field as done by Ronsin and Perrin [4]. The amplitude A remains, as in all linear bifurcation analyses, undetermined. To determine the onset of the oscillatory instability the analyses $A/L\to 0$ (at fixed L) must be done in the numerical realization (see Sec. V).

III. THE THERMOELASTIC PROBLEM

The mechanical equilibrium equations take the quasistatic form

$$\sigma_{ij,i}=0 \tag{10}$$

by using the Einstein sum convention with $i,j=x,y$. The comma followed by index j denotes the partial derivative with respect to the coordinate j. The constitutive equations for thermoelastic isotropic materials are

$$\sigma_{ij}=\frac{E}{1+\nu}\left(\epsilon_{ij}+\frac{\nu}{1-2\nu}\epsilon_{kk}\delta_{ij}\right)-\frac{E}{1-2\nu}\alpha(T-T_R)\delta_{ij}. \tag{11}$$

E, ν, and α are Young's modulus, Poisson number, and thermal expansion coefficient, respectively. T is the temperature and T_R the reference temperature. In this case T_R can be arbitrarily chosen due to traction free boundaries [see Eq. (13)]. The infinitesimal strain ϵ_{ij} is defined by

$$\epsilon_{ij}=\frac{1}{2}(u_{i,j}+u_{j,i}), \tag{12}$$

where u_i is displacement in direction i. The boundaries of the slab as well as the crack faces are traction free

$$\sigma_{ij}n_j=0, \tag{13}$$

with n_j being an outward unit vector normal to the boundaries or crack faces.

The interaction between mechanical and thermal fields is negligible because of small deformation and quasistatical crack propagation. At the onset of oscillation $A/L\to 0$ the crack does not influence the temperature field [18].

IV. THE TEMPERATURE FIELD

First we want to have a closer look at the temperature distribution because of its crucial importance for the thermomechanical problem. The second derivatives of the temperature distribution are responsible for the induced stress field. In literature a stationary temperature field is commonly assumed which follows from the differential equation for the stationary heat conduction with idealized boundary conditions.

Most works [6,9,10,15–19,23] used a theoretical temperature field determined only by the thermal diffusion length $l_1=D/v$ and without consideration of the gap length h. In the moving coordinate system (see Fig. 1) that reads

$$T(x,v)=T_B+\Delta T[1-e^{-x/l_1}]\theta(x), \tag{14}$$

where θ is the Heaviside function and T_B is the temperature of the bath. The temperature function (14) is the solution of the idealized, one-dimensional stationary heat equation

$$T_{,xx}+T_{,x}/l_1=0$$

with the boundary conditions

$$T(x=0)=T_B \quad \text{and} \quad T(x\to\infty)=T_B+\Delta T.$$

This temperature profile is intended for the theoretical limiting case of infinite gap h and for very high velocities.

In order to extend the range of comparison between theory and experiment to low velocities, Ronsin *et al.* [2] suggested a more realistic temperature profile

$$T(x,v)=T_B+\Delta T\left[\frac{1-e^{-x/l_1}}{1-e^{-h/l_1}}\theta(x)\theta(h-x)+\theta(x-h)\right] \tag{15}$$

which fulfills the boundary conditions $T(x=0)=T_B$ and $T(x=h)=T_B+\Delta T$. This temperature field is controlled by the gap length h for low velocities and by the thermal diffusion length $l_1=D/v$ for high velocities.

Two important simplifications are made in the above theoretical temperature fields (14) and (15). The temperature of the bath is reached in the slab immediately at the boundary with the gap. In addition, the heat exchange with the air surroundings is not considered, which is essential in the range of real velocities as in the experiments.

Already in 1995, Ronsin *et al.* [2] discussed the temperature distribution in detail and called into question the validity of the idealized temperature profile. They found out that the temperatures of the bath and the oven are not reached exactly at the cold front and at the hot front, respectively, as assumed in the theoretical temperatures (14) and (15). The real tem-

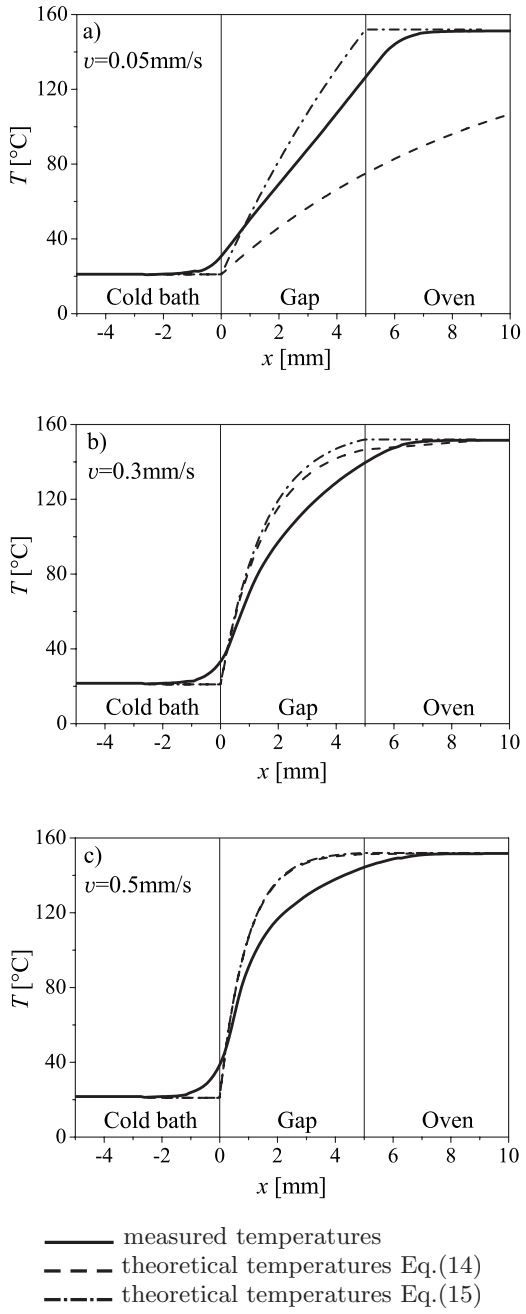

FIG. 2. Comparison of theoretical and experimental temperature distributions revealing large differences. v is slab velocity. Experimental curves are measured by Ronsin and Perrin (Fig. 2 in Ref. [4], after correction of an obvious mix-up concerning the curves a and c).

perature profile, differing from the theoretical ones, shows two smooth changes with characteristic lengths of 1 mm to 2 mm (compare Fig. 2). The theoretical temperature profiles overestimate the second derivatives and consequently yield essentially higher fracture energy. Therefore, they recommended to use the real experimental thermal profile.

Nevertheless the theoretical temperatures (14) and (15) were further used in the literature and even more or less good agreement with experimental results was reported. In Fig. 2 we do now compare the temperature distributions as measured by Ronsin and Perrin [4] with the theoretical ones (14) and (15) for the velocities $v=0.05$ mm s^{-1} (a), $v=0.3$ mm s^{-1} (b), and $v=0.5$ mm s^{-1} (c). It is evident that the theoretical curves do not match the measured curves at all, not only near the cold front and heat front as noticed by Ronsin and Perrin [2] but moreover also within the gap. Significant differences can be seen not only at low velocities $v=0.05$ mm s^{-1} but also at higher velocity $v=0.5$ mm s^{-1}.

As mentioned in the Introduction, by using the local criterion for the oscillating instability (5) and the theoretical temperature function (15) Bouchbinder *et al.* [12] recently obtained a rather good agreement with the experiments in Ref. [2]. In view of the "wrong" temperatures used in their calculation it is to be expected that this local criterion fails with "correct" temperature distributions, which will also be shown in the following. In our analyses we do not use the theoretical temperatures (14) and (15) but the measured ones.

V. NUMERICAL RESULTS AND COMPARISON WITH EXPERIMENTS

Equations (8) and (9) can be solved numerically by variation of the crack path parameters λ/L and a/L. In order to calculate the critical width L_{osc} for oscillating instability, the fracture toughness K_{Ic} is needed. Unfortunately, K_{Ic} and the fracture energy $\Gamma=K_{\mathrm{Ic}}^2/E$ of soda-lime glass are uncertain parameters [12]. In general, they vary with the temperature, the velocity, and particularly with the humidity [4,34,35]. Nevertheless, Bouchbinder *et al.* [12] used a constant value $\Gamma=3.75$ J m^{-2} chosen to best fit the experimental data at the onset of the straight crack propagation. Note that this high value for the fracture energy was calculated with the theoretical temperatures (15) and is accordingly not adequate as discussed above.

As will be discussed below we do not use Eq. (9) and a value for K_{Ic} but we take the critical width $L=L_{\mathrm{osc}}$ obtained experimentally by Ronsin and Perrin (Fig. 15 in Ref. [4]) at $\Delta T=135$ K for a velocity v at which they also measured the temperature field (see Fig. 2). That means that all experimental conditions are completely taken into account in our calculation model. This allows a_{osc} and λ_{osc} to be determined from Eq. (8) and K_{Ic} from Eq. (9).

In the following we will examine the cases with v between 0.05 mms^{-1} and 0.5 mms^{-1} extracted from Fig. 15 in Ref. [4], which are listed in Table I. Because Ronsin and Perrin measured temperature fields for only three velocities $v=0.05$, 0.3, and 0.5 mm s^{-1}, we determine the temperature fields for other velocities within this range by quadratic interpolation in v. In Table I, "m" and "i" stand for measured temperatures and interpolated ones, respectively.

We used the finite element (FE) code ANSYS [36] for the fracture mechanics analyses. Isoparametric quadratic plane stress elements were employed with collapsed quarter-point singular elements right around the crack tip to generate the square-root stress singularity. The stress intensity factors were calculated from the stresses (1) or from the displacements in the vicinity of the crack tip according to linear elastic fracture mechanics. The following material parameters were used for soda-lime glass: thermal diffusivity D

TABLE I. Experimental cases chosen from Figs. 2, 15, and 16 in Ref. [4], to be considered in the following.

v [mm s^{-1}]	0.05	0.063	0.113	0.15	0.2	0.25	0.3	0.375	0.45	0.5
L [mm]	13.9	14.1	14.1	14.1	14.2	14.2	13.5	12.5	11.5	10.8
Temperature distribution[a]	*m*	*i*	*i*	*i*	*i*	*i*	*m*	*i*	*i*	*m*

[a]*m*: measured; *i*: derived from measured data by interpolation.

$=0.5$ mm^2 s^{-1}, Young's modulus $E=72$ GPa, and thermal expansion coefficient $\alpha=0.77\times10^{-5}$ K^{-1} [2]. Preliminary studies showed that the influence of A/L on the solution can be neglected for sufficiently small $A/L<1/200$. Therefore, the determination of limiting values for $A/L\to0$ at the transition between straight and oscillatory crack paths is not necessary.

First we consider the idealized case $v\to\infty$ [i.e., the normalized diffusion length $D/(vL)\to0$] where there is a step in the temperature field at the cold front $x=0$. The only characteristic length is the width L. Also in this unrealistic case the ratios a_{osc}/L and λ_{osc}/L can be calculated from Eq. (8) solely. Figure 3 shows the analysis results $k_{\mathrm{II}}L/A$ of the sine-phase (β_1) and the cosine-phase (α_1) by variation λ/L for this case. Equation (8) are satisfied at $a_{\mathrm{osc}}/L=0.047$ and $L/\lambda_{\mathrm{osc}}=7.53$ ($\lambda_{\mathrm{osc}}/L=0.133$). As can be seen in Fig. 3, these parameters also fulfill the AP criterion (5). In this unrealistic, theoretical case the global bifurcation criterion and the local AP criterion provide the same result.

For a realistic finite diffusion length $D/(vL)$ as in experiments by Ronsin and Perrin [4], the results of the global criterion (8) differ from that of the AP criterion (5). This is shown in Figs. 4(a) and 4(b) for $D/(vL)=0.0926$ ($v=0.5$ mm s^{-1}). While the results of our global bifurcation criterion $a_{\mathrm{osc}}/L=0.271$ and $\lambda_{\mathrm{osc}}/L=0.385$ [Fig. 4(a)] are in good agreement with the experimental one $(\lambda/L)_{\mathrm{exp}}=0.37$, the local AP criterion yields $a_{\mathrm{AP}}/L=0.268$ and $\lambda_{\mathrm{AP}}/L=0.465$ [Fig. 4(b)].

As one can see in Fig. 4(b), k_{II} does not vanish for the cosine-phase at the solution of the AP criterion. Inserting $\alpha_1=k_{\mathrm{II}}(\varphi=\frac{\pi}{2})\frac{L}{A}>0$ and $\beta_1=k_{\mathrm{II}}(\varphi=0)\frac{L}{A}=0$ into Eq. (7) gives $k_{\mathrm{II}}(\varphi)=\alpha_1\frac{L}{A}\sin\varphi$. This means that, with $\alpha_1>0$ at the solution of the AP criterion, the crack will always turn inward, which results in a damped oscillation approaching a straight line. Such behavior ends as soon as the critical value $L/\lambda_{\mathrm{osc}}=2.6$ is reached, where $k_{\mathrm{II}}=0$ for all φ because of $\alpha_1=\beta_1=0$. This is an argument for Eq. (8) being a global bifurcation criterion for oscillatory crack path instability.

Figures 5 and 6 show two further cases $v=0.45$ mm s^{-1} [$D/(vL)=0.0966$] and $v=0.3$ mm s^{-1} [$D/(vL)=0.123$], respectively. The AP criterion (5) leads to higher wavelength with realistic temperatures. For $v\leq0.3$ mms^{-1} even no re-

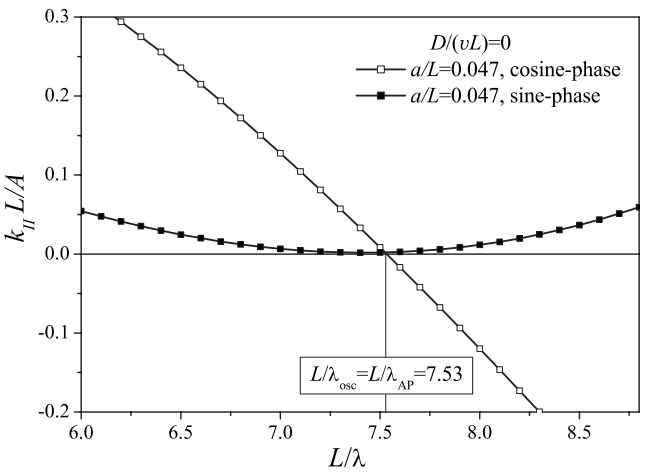

FIG. 3. Analysis result obtained with an idealized abrupt temperature transition $D/(vL)\to0$: k_{II} vanishes for both cosine-phase and sine-phase at $a_{\mathrm{osc}}/L=0.047$ and $\lambda_{\mathrm{osc}}/L=0.133$, where the condition $\partial k_{\mathrm{II}}/\partial\lambda=0$ is also satisfied. In this unrealistic, theoretical case the AP criterion (5) gives the same result as the global criterion (8).

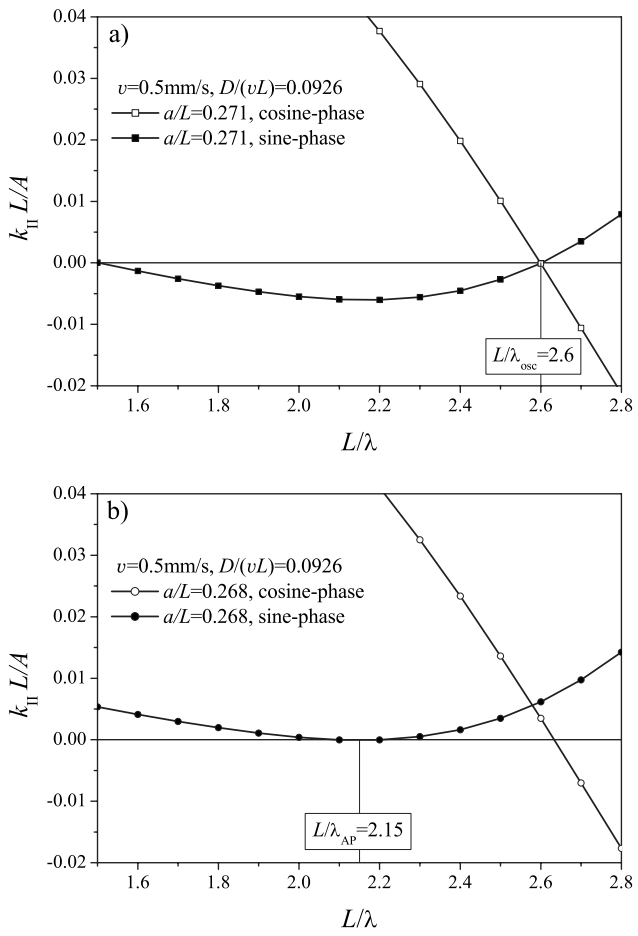

FIG. 4. Analysis result obtained with the temperature distribution measured by Ronsin and Perrin [4] for $v=0.5$ mm s^{-1} and $L=L_{\mathrm{osc}}=10.8$ mm: (a) global criterion: k_{II} vanishes for both cosine-phase and sine-phase at $a_{\mathrm{osc}}/L=0.271$ and $\lambda_{\mathrm{osc}}/L=0.385$. (b) The AP criterion (5) gives incorrect result $a_{\mathrm{AP}}/L=0.268$ and $\lambda_{\mathrm{AP}}/L=0.465$, where $k_{\mathrm{II}}\neq0$ for cosine-phase.

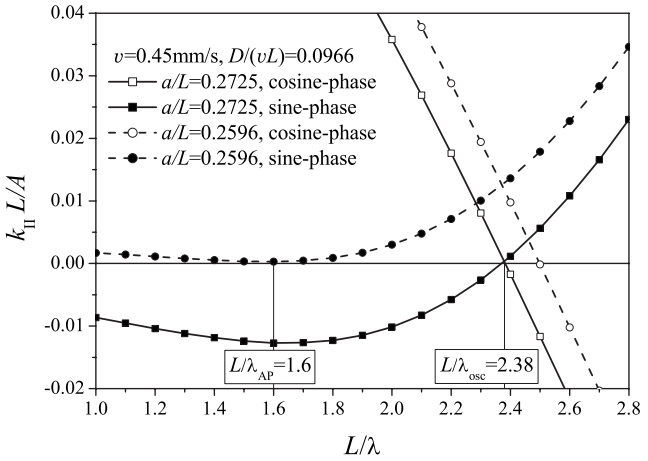

FIG. 5. Analysis result obtained with the interpolated temperatures from the measured ones by Ronsin and Perrin [4] for $v=0.45$ mm s^{-1} and $L=L_{osc}=11.5$ mm: The global criterion (8) yields $a_{osc}/L=0.2725$ and $\lambda_{osc}/L=0.42$ agreeing very well with experiments. The AP criterion (5) gives $a_{AP}/L=0.2596$ and $\lambda_{AP}/L=0.625$ which exceeds the experimental value (see Fig. 7).

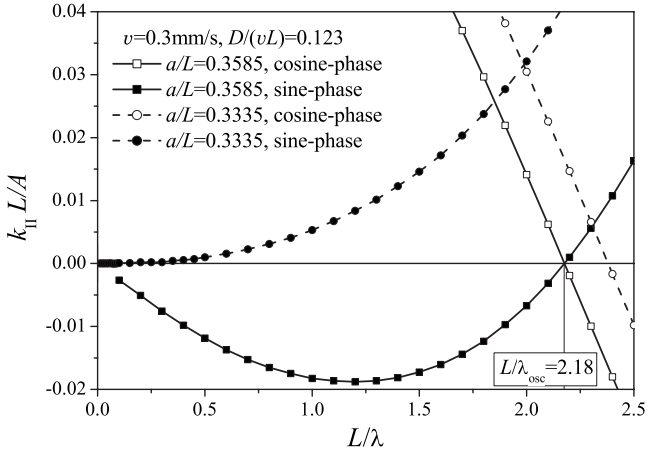

FIG. 6. Analysis result obtained with the temperatures measured by Ronsin and Perrin [4] for $v=0.3$ mm s^{-1} and $L=L_{osc}=13.5$ mm: The global criterion (8) yields $a_{osc}/L=0.3585$ and $\lambda_{osc}/L=0.4587$ agreeing very well with experiments (see Fig. 7). The AP criterion (5) gives no result.

sult is available with this criterion, the wavelength λ_{AP} seems to shift to infinity (Fig. 6).

In Fig. 7 the critical wavelengths of the crack at the onset of the oscillating as a function of the normalized diffusion length are represented as results of the global bifurcation criterion (8) and the local AP criterion (5) in comparison with the experimental ones by Ronsin and Perrin [4]. While the results of the global criterion (△,▽) agree excellently with the experiments (▲) for all cases, the AP criterion (□, ◇) always yields greater wavelengths, at least an order of magnitude greater for $D/(vL)\geq 0.123$.

Ronsin and Perrin (Fig. 16 in Ref. [4]) interpreted the experimental results by two straight lines. The two lines as limits are also confirmed by our numerical analyses: in the high velocity regime ($D/v \ll h$), the wavelength λ varies lin-

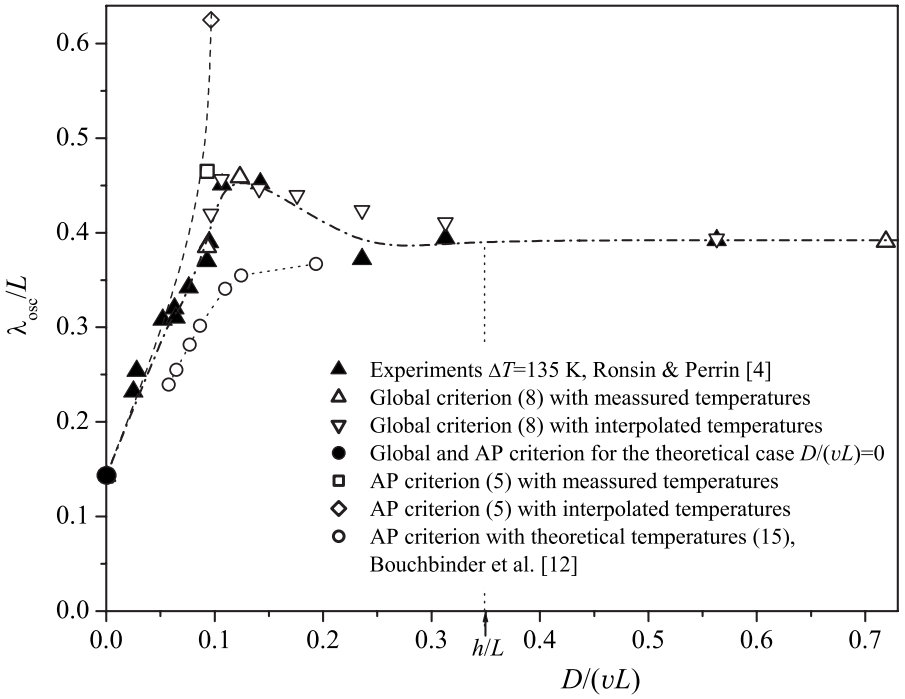

FIG. 7. Comparison of the analysis results obtained with the measured (△,□) and interpolated (▽, ◇) temperatures with experimental results of Ronsin and Perrin (Figs. 15 and 16 in Ref. [4]). The temperature profiles and the widths $L=L_{osc}$ are taken from Ref. [4] (see also Table I). The experimental results (▲) are connected with a dash-dotted line as an aid for the eyes. The results of the global criterion (△,▽) agree very well with experiments. In contrast, the Adda-Bedia and Pomeau criterion (5) (□, ◇, connected with a dashed line) yields no agreement with the experimental results for realistic diffusion length D/v. The results of Bouchbinder *et al.* [12] (○···○) are based on the theoretical temperatures (15) and constant fracture energy $\Gamma=3.75$ J m^{-2}.

early with the diffusion length D/v, while in the low velocity regime ($D/v > h$) the wavelength λ is constant and controlled by h ($D/v = h$ is indicated on the abscissa in Fig. 7). The intersection point of the two straight lines as the transition from high velocity regime to low velocity regime (Fig. 16 in Ref. [4]) is only idealized. In our opinion, the more realistic transition region between these two limits is nonmonotonic as the dash-dotted line in Fig. 7 shows a maximum between $D/(vL)=0.1$ and $D/(vL)=0.14$. The experimental results as well as the results of our global criterion show this nonmonotonic behavior in this region. This is caused, possibly, by the complicated actual temperature distributions in Fig. 2.

Bouchbinder *et al.* [12,38] replace the principle of local symmetry (2) by a so-called dynamic law proposed by Hodgdon and Sethna [37]:

$$\frac{\partial \theta}{\partial t} = -fK_{\mathrm{II}}, \tag{16}$$

where f is a positive material parameter. Since $\partial/\partial t = v\,\partial/\partial s$ (s: crack path length), Eq. (16) means that the curvature is proportional to K_{II}, contrary to Eq. (3).

Now we apply Eq. (16) globally to the entire oscillation crack path. After Ref. [38], the parameter f can be expressed by $v/[l(v)K_{\mathrm{I}}]$, where $l(v)$ is some length related to the process zone, which makes

$$\frac{\partial \theta}{\partial s} = -\frac{1}{l(v)}\frac{K_{\mathrm{II}}}{K_{\mathrm{I}}}. \tag{17}$$

With $\partial/\partial s \approx \partial/\partial x$ and $\partial\theta/\partial s \approx \partial^2 y/\partial x^2$ for $\partial y/\partial x \ll 1$ we obtain with Eqs. (6) and (7)

$$A\left(\frac{2\pi}{\lambda}\right)^2 \sin\varphi = \frac{1}{l(v)}\frac{A}{L}\frac{\alpha_1 \sin\varphi + \beta_1 \cos\varphi}{k_{\mathrm{I}}(a/L, D/(vL))}. \tag{18}$$

Equation (18) can be fulfilled along the entire oscillation crack path for all φ if

$$\alpha_1 = \left(\frac{2\pi}{\lambda}\right)^2 l(v) L k_{\mathrm{I}}\left(\frac{a}{L}, \frac{D}{vL}\right), \quad \beta_1 = 0. \tag{19}$$

Considering the tendencies of $\alpha_1(a/L, D/(vL))$ and $\beta_1(a/L, D/(vL))$ in Figs. 5 and 6, the solution of Eq. (19) gives larger critical wavelengths than the principle of local symmetry does. However, since the scale of the process zone is small compared to the other lengths, Eq. (19) corresponds to our global bifurcation criterion (8) in a very good approximation. It can be concluded that Eq. (16) gives practically the same remarkably good agreement between theory and experiments in Fig. 7. However, it must be pointed out that it has to be applied globally to the entire oscillation crack path but not only locally to the sine-phase as in Ref. [12] which gives the AP criterion with poor or no agreement with the experiment for small velocities (squares in Fig. 7).

As another result of the global criterion, we get the mode I SIF $K_{\mathrm{I}} = K_{\mathrm{I}}(v)$ at the onset of the oscillatory instability with a_{osc}/L from Eq. (8). As mentioned above we did not use Eq. (9) but took the critical, experimentally observed width $L = L_{\mathrm{osc}}$ from Ref. [4]. In Fig. 8 the calculated mode I SIF $K_{\mathrm{I}}(v)$ of soda-lime glass is plotted vs velocity v showing a decrease of $K_{\mathrm{I}}(v)$ with increasing v which seems to be unexpected at first glance and will be discussed in the following.

In order to understand this dependence we do not identify $K_{\mathrm{I}}(v)$ with $K_{\mathrm{I}c}$ in Eqs. (4) and (9) because for slow velocities as in the experiments the cracks do not grow critically but subcritically with $K_{\mathrm{I}}(v) < K_{\mathrm{I}c}$ as in Ref. [34]. The dependence of the velocity on K_{I} is usually expressed by a power law (see, e.g., Ref. [34]):

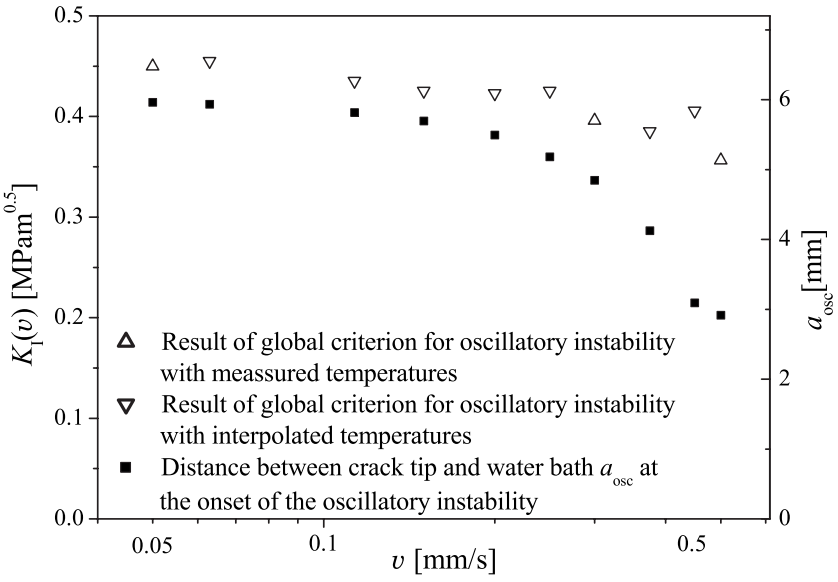

FIG. 8. Mode I SIF $K_{\mathrm{I}}(v)$ at the onset of the oscillatory instability as a result of the global criterion calculated with the measured ($\triangle$) and interpolated ($\triangledown$) temperatures. The velocity affects K_{I} also indirectly through the humidity and the temperature at the crack tip which both depend on the distance between the crack tip and the water bath a_{osc}.

$$v = BK_I^n. \tag{20}$$

The power n had been measured to be approximately 16 for soda-lime glass [34]. B is another material parameter. With constant B, K_I would increase with the nth root of v. However, B depends on temperature and humidity at the crack tip, which depend on the distance a and hence on v, and therefore the relation between K_I and v may be quite different in the present experimental situation. The effect of water on fracture of soda-lime glass was discussed by Ronsin and Perrin [4] on a molecular level. Water tends to loosen the Si-O-Si bonds, which results in higher B and hence lower K_I with given v according to Eq. (20). This tendency was confirmed experimentally by Kocer and Collins (Fig. 7 in Ref. [34]).

In the experiments by Ronsin and Perrin [4], with given dipping velocity v, temperature field, and slab width L, Eq. (20) is fulfilled for straight and small amplitude oscillating crack propagation by an appropriate distance a between the crack tip and the cool front (see Fig. 1). The distance a controls the crack tip temperature and humidity in the factor B in Eq. (20). From the global bifurcation criterion (8) with the measured value $L=L_{osc}$, the distance a_{osc} in Fig. 8 has been calculated. It decreases with increasing v, which makes higher humidity and lower temperature at the crack tip. Evidently, the influence of humidity outweighs that of temperature. This makes lower K_I with higher v in the present case. Our calculated $K_I(v)$ values are not unreasonable with respect to Fig. 7 in Ref. [34] if one considers that $K_I(v)$ was determined by Kocer and Collins for ambient temperature. The variation of $K_I=K_I(v)$ in Fig. 8 also points out that the calculation with a constant value for the fracture energy independent of experimental conditions as done in Ref. [12] is problematic.

VI. CONCLUSIONS

We have derived a *global bifurcation criterion* for the transition from straight to quasistatic oscillating crack propagation in an isotropic material from pure mode I stress fields at the crack tip ($K_{II}=0$) on the entire smooth, oscillating crack path. As shown before for other problems of directional crack path instability [24,39], the entire crack path has to be analyzed for such bifurcation problems. For a small-amplitude sine-shaped crack path at the transition, it is shown to be sufficient to postulate $K_{II}=0$ for two phases of the crack path only, instead of for any crack tip position.

As discussed by Ronsin and Perrin [4] the critical sample width L_{osc} and the critical wavelength λ_{osc} of the crack path at the oscillating instability depend sensitively on the temperature field and on the fracture toughness which varies, e.g., with propagation velocity, temperature, and humidity. It has been shown that the theoretical temperature functions (14) and (15) as usually employed in the literature are insufficient approximations for the present purpose. Therefore, the real temperature distributions have to be used. By employing the measured temperature field at $\Delta T=135$ K and the experimentally observed width $L=L_{osc}$ which implicitly carries information on fracture toughness, the critical wavelengths λ_{osc} derived by our global bifurcation criterion agree remarkably well with those obtained experimentally.

Local bifurcation criteria cannot predict the oscillatory instability correctly. In contrast to some explanations in the literature the Cotterell and Rice solution [21] is universal, i.e., also for finite geometry. However, it is valid only for a small amount of crack growth after a disturbance compared to a characteristic length [24,40]. In this validity range of the Cotterell and Rice solution it is not possible to decide whether the oscillation increases or decreases. This is the correct explanation why the T criterion does not work for the oscillating instability, not because of the finite geometry as commonly given in the literature [2,23].

The local bifurcation criterion used in Refs. [10], [12] which considers only one crack tip position, i.e., one phase $\varphi=0$ of the sine function, yields approximate results only for very high velocities but no oscillatory instability at all for low velocities (see Fig. 7).

It has been shown in this paper and in Ref. [33] that quasistatic crack propagation with smooth crack trajectory in isotropic materials can be described by the principle of local symmetry $K_{II}=0$. The condition of $K_{II}=0$ being fulfilled along the entire crack path provides critical wavelengths which agree remarkably well with experiments. The "new dynamical" approach with $K_{II}\neq 0$ and $K_{II}\ll K_I$ as used in Ref. [12] yields about the same result for the present case but only if applied to the entire oscillating crack path. Its superiority to the conventional approach as claimed in Refs. [12,38] would have to be demonstrated with suitable experiments.

ACKNOWLEDGMENTS

The authors thank A. Gerbatsch for reading the manuscript and helpful discussion and one reviewer for many helpful comments and questions for improving the paper. The support for this work by the Deutsche Forschungsgemeinschaft (DFG) under Contract No. Ba 1561/4 and Ba 1411/11 is greatly acknowledged.

[1] A. Yuse and M. Sano, Nature (London) **362**, 329 (1993).
[2] O. Ronsin, F. Heslot, and B. Perrin, Phys. Rev. Lett. **75**, 2352 (1995).
[3] O. Ronsin and B. Perrin, Europhys. Lett. **38**, 435 (1997).
[4] O. Ronsin and B. Perrin, Phys. Rev. E **58**, 7878 (1998).
[5] A. Yuse and M. Sano, Physica **108**, 365 (1997).
[6] B. D. Ferney, M. R. DeVary, K. J. Hsia, and A. Needleman, Scr. Mater. **41**, 275 (1999).
[7] H. Furukawa, Prog. Theor. Phys. **90**, 949 (1993).
[8] Y. Hayakawa, Phys. Rev. E **49**, R1804 (1994).
[9] M. Marder, Phys. Rev. E **49**, R51 (1994).
[10] M. Adda-Bedia and Y. Pomeau, Phys. Rev. E **52**, 4105 (1995).

[11] B. Yang and K. Ravi-Chandar, J. Mech. Phys. Solids **49**, 91 (2001).
[12] E. Bouchbinder, H. G. Hentschel, and I. Procaccia, Phys. Rev. E **68**, 036601 (2003).
[13] Y. Sumi, S. Nemat-Nasser, and L. M. Keer, Eng. Fract. Mech. **22**, 759 (1985).
[14] Y. Sumi and Y. Mu, Mech. Mater. **32**, 531 (2000).
[15] S. I. Sasa, K. Sekimoto, and H. Nakanishi, Phys. Rev. E **50**, R1733 (1994).
[16] H.-A. Bahr, A. Gerbatsch, U. Bahr, and H.-J. Weiss, Phys. Rev. E **52**, 240 (1995).
[17] H.-A. Bahr, U. Bahr, A. Gerbatsch, I. Pflugbeil, A. Vojta, and H.-J. Weiss, in *Fracture Mechanics of Ceramics 11*, edited by R. Bradt, D. Hasselman, D. Munz, M. Sakai, and V. Y. Shevchenko (Plenum, New York, 1996), Vol. 11, pp. 507–522.
[18] A. Gerbatsch, Ph.D. thesis, Technische Universität Dresden, 1997.
[19] V. Mühle, Ph.D. thesis, Technische Universität Dresden, 2000.
[20] R. Niefanger, V.-B. Pham, G. A. Schneider, H.-A. Bahr, H. Balke, and U. Bahr, Acta Mater. **52**, 117 (2004).
[21] B. Cotterell and J. R. Rice, Int. J. Fract. **16**, 155 (1980).
[22] M. L. Williams, J. Appl. Mech. **24**, 109 (1957).
[23] M. Adda-Bedia and M. Ben Amar, Phys. Rev. Lett. **76**, 1497 (1996).
[24] V.-B. Pham, H.-A. Bahr, U. Bahr, T. Fett, and H. Balke, Int. J. Fract. **141**, 513 (2006).
[25] M. Amestoy and J. B. Leblond, Int. J. Solids Struct. **29**, 465 (1992).
[26] G. I. Barenblatt and G. P. Cherepanov, Phys. Met. Metallogr. **25**, 1654 (1961).
[27] G. P. Cherepanov, Phys. Met. Metallogr. **27**, 150 (1963).
[28] F. Erdogan and G. C. Sih, J. Basic Eng. **85**, 519 (1963).
[29] R. V. Gol'dstein and R. L. Salganik, Int. J. Fract. **10**, 507 (1974).
[30] S. Melin, Int. J. Fract. **30**, 103 (1986).
[31] K. B. Broberg, *Crack and Fracture* (Academic Press, San Diego, 1999).
[32] M. Marder, Europhys. Lett. **66**, 364 (2004).
[33] S. L. dos Santos e Lucato, H.-A. Bahr, V.-B. Pham, D. C. Lupascu, H. Balke, J. Rödel, and U. Bahr, J. Mech. Phys. Solids **50**, 2333 (2002).
[34] C. Kocer and R. E. Collins, J. Am. Ceram. Soc. **11**, 2585 (2001).
[35] S. M. Wiederhorn, A. Dretzke, and J. Rödel, J. Am. Ceram. Soc. **85**, 2287 (2002).
[36] ANSYS, revision 10, Swanson Analysis Systems, Inc., Houston, 2005.
[37] J. A. Hodgdon and J. P. Sethna, Phys. Rev. B **47**, 4831 (1993).
[38] E. Bouchbinder and I. Procaccia, Phys. Rev. Lett. **98**, 124302 (2007).
[39] S. Melin, Int. J. Fract. **114**, 259 (2002).
[40] S. Melin, Int. J. Fract. **23**, 37 (1983).